PHYSICAL REVIEW B VOLUME 27, NUMBER 4 15 FEBRUARY 1983

Inelastic neutron scattering studies of vibrational excitations of hydrogen in Nb and Ta

J. Eckert, J. A. Goldstone, and D. Tonks
Los Alamos National Laboratory, Los Alamos, New Mexico 87545

D. Richter
Institut für Festkörperforschung, Kernforschungsanlage Jülich, D-517 Jülich, Federal Republic of Germany

(Received 20 August 1982)

Inelastic incoherent neutron scattering techniques have been used to study the optic vibrations in hydrides of Nb and Ta for hydrogen concentrations between 44 and 49 at. % in the case of Nb and 42 at. % for Ta and at temperatures between 10 and 295 K. In all cases the first harmonic of the singlet fundamental vibration could be observed with an anharmonic shift of 3—5 % to lower energies. In addition, evidence is presented for the first time of a combination band corresponding to the simultaneous excitation of the singlet and doublet fundamental vibration corresponding to out-of-plane and in-plane motion, respectively, of the proton on its tetrahedral site. These modes are coupled by anharmonic interactions which are described by a three-dimensional anharmonic-oscillator model of tetragonal symmetry ($\bar{4}2m$) appropriate to hydrogen in bcc metals. This analysis using both the present data as well as previous work by other authors gives a consistent picture of anharmonicity in the bcc metal hydrides. In addition, splittings and/or broadening of the observed vibrational peaks for some concentrations or temperatures could be correlated with recent, new information on the high-concentration, low-temperature portion of the NbH_x phase diagram.

I. INTRODUCTION

The possibility of gaining important information on the hydrogen-metal interaction by studying the optic modes in metal hydrides with the use of inelastic neutron scattering techniques has recently attracted considerable attention.[1–7] While the measurement of complete phonon dispersion relations can provide significantly more detail on the dynamics than that of the optic branches alone, the former is restricted by the availability of large single crystals, and has therefore been possible in only a few cases among metal hydrides.[2,8–11] The reason for this is that the loading of a single crystal with hydrogen tends to expand the lattice too much for the crystal to retain its integrity. Particularly in cases where the optic branches show no dispersion, their measurement can be performed using polycrystalline samples and the results can be interpreted by regarding the protons as isolated Einstein oscillators.[2,3,5] Such has been shown to be the case for Nb (Ref. 8) by measurements of phonon dispersion relations and should be applicable to Ta as well. This is in contrast to the fcc hydrides of Pd (Ref. 9) and Ce (Refs. 10 and 11) where significant interaction between hydrogen atoms is indicated. Further details on the shape of the hydrogen-metal potential can then be obtained in the former cases by determining the isotopic shift on the local-mode frequencies as well as the higher harmonics of the oscillator transitions. Anharmonicity in the potential is then reflected by a deviation of these quantities from the harmonic values. Some previous studies[3,5] have in fact utilized a simple one-dimensional anharmonic-oscillator model[12] for each component of the hydrogen vibration to analyze the data with good success in terms of a single anharmonicity parameter.

With the presence of anharmonicity as well as the fact that the β phase of the bcc hydrides shows an orthorhombic distortion, it is no longer obvious that the x, y, and z motions of the proton in its potential well are still decoupled. A more general approach to this problem would be to describe the proton as a three-dimensional anharmonic oscillator and apply the operations appropriate to the tetragonal site symmetry $\bar{4}2m$ of the bcc structure to the Hamiltonian to find the nonzero terms to fourth order in the displacements. The effect of the orthorhombic distortion can then be included at a later stage in a manner to be discussed below. However, such a multiparameter model for anharmonicity requires more information on the vibrational spectrum of hydrogen in metals than what normally has been obtained in experiments of this type. With the exception of more recent work,[3–6] former inelastic neu-

tron scattering studies[2] were not generally of sufficient accuracy to test seriously models for anharmonicity. Furthermore, most experiments performed on reactor-based neutron sources could not be extended to sufficiently large energy transfers for the measurements of the higher harmonics as well as possible combination bands of the oscillator transitions because of the rapid falloff of the reactor neutron spectrum at large energies. Thus, in order to have even a chance to test more sophisticated models for the hydrogen potential in these systems, experimental data have to be both of high accuracy as well as extend to larger energy transfers.

A final introductory remark concerns the determination of the isotope effect on the vibrational spectrum of the metal hydrides, which represents an important piece of information for the determination of the anharmonicity parameters. Typically the comparison between a hydride and deuteride have not been made on samples of the same concentration.[4,5] While the overall concentration dependence of the local-mode frequencies in the bcc hydrides may be slight,[13] differences are significant at the few-percent level of the anharmonic shifts[2–4] that have been observed. In addition, complications may arise from the very complex phase diagram[14] (particularly at higher hydrogen concentrations) which has recently been determined for NbH_x for temperatures below 295 K. The reason for this is that the local environment around the tetrahedral hydrogen site may be different in the various phases and that, therefore, different local-mode frequencies may arise. If two or more such phases coexist in a region of the phase diagram, the local-mode peaks may be broadened, and the mean frequency of such a peak cannot readily be compared with that of a single-phase sample. These considerations are less important in the low-concentration portion of the phase diagram, which is the focus of some of the recent studies.[3,4]

The present neutron scattering studies, therefore, were undertaken to address the three points concerning previous work on the systems mentioned above. We will first discuss a more general model of a three-dimensional anharmonic oscillator with tetragonal symmetry. Extensive data taken at a new accelerator-based neutron source reaching energy transfers greater than 300 meV will then be presented and analyzed along with previous data using this model. Finally, the observed line shapes will be related to newly available information on the NbH_x phase diagram at low temperatures.

II. THEORY

The vibrational spectrum of a local harmonic oscillator located on a tetrahedral site in the bcc structure (site symmetry $\bar{4}2m$ or D_{2d}) and interacting only with its four nearest-neighbor atoms consists of two sets of equally spaced transition lines. One of those sets results from vibrations in the plane formed by two axes of the cubic structure (hereby defined to be the x and y axes) and the hydrogen site, and these lines are, therefore, doubly degenerate. The lower-energy transitions for each harmonic-oscillator level correspond to motions out of the plane, i.e., along the z direction. In the absence of anharmonic coupling between the in-plane and out-of-plane motions it is possible to treat the singlet motion as a one-dimensional anharmonic oscillator with a single anharmonicity parameter. This is the approach taken in some previous studies.[3,5]

More generally, one may describe the motion of the hydrogen as a three-dimensional anharmonic oscillator and use the appropriate symmetry operations to reduce the number of terms in the Hamiltonian. Terms of the third and fourth order of the displacements can then be treated as perturbations on the harmonic frequencies described below. Cubic anharmonicities make no contribution in a first-order perturbation theory and are, therefore, treated to second order, while quartic anharmonicity is included by first-order perturbation theory. The resulting renormalized vibrational frequencies can then be compared with experimental data on the higher harmonics as well as the isotope effect to extract values for the anharmonicity parameters.

The use of symmetry considerations reduces the number of cubic and quartic anharmonic terms to a total of five, as may be shown by formal group theory. Tinkham[15] shows the appropriate character table for $\bar{4}2m$ symmetry (see p. 328), but the row labels "x^2-y^2" and "xy" need to be switched. More elementary considerations lead to the same results. For example, mirror-plane reflections in the plane of the H-site bcc cube face (x,z plane), or in the y,z plane are point-symmetry operations of the H site which change the sign of the y or x normal-mode coordinate, respectively, but not that of the z normal-mode coordinate. Hence, any term of the potential energy involving an odd power of x and/or y is zero since its sign is reversed by one of the reflections. By this and similar considerations, and choosing the H site to have the maximum z coordinate in the bcc cube face, one can eliminate all but the following cubic and quartic terms in the Hamiltonian H_1:

$$H_1 = ez(x^2-y^2)+c_{4,z}z^4+c_{4,x}(x^4+y^4) + fx^2y^2+gz^2(x^2+y^2)\,. \quad (1)$$

Here the subscript 4 on $c_{4,z}$ and $c_{4,y}$ indicates a

quartic term, while the subscripts z and x refer to the mode in question, i.e., singlet or out-of-plane and doublet or in-plane, respectively. This is the sense in which these subscripts are henceforth used. It is straightforward to work out the perturbation theory and obtain the excitation energies $e_{lmn}=E_{lmn}-E_{000}$, where E_{lmn} is the perturbed energy of the vibrational state corresponding to the l,m,n harmonic level, i.e., that with l, m, and n vibrational excitations in modes z, x, and y, respectively,

$$e_{100}=\hbar\omega_z-\lambda'-\lambda''+12c_{4,z}\epsilon_z^2+4g\epsilon_z\epsilon_x\ , \tag{2}$$

$$e_{010}=e_{001}=\hbar\omega_x-\lambda-\lambda''+12c_{4,x}\epsilon_x^2 +2f\epsilon_x^2+2g\epsilon_z\epsilon_x\ , \tag{3}$$

$$e_{200}=2\hbar\omega_z-2\lambda'-2\lambda''+36c_{4,z}\epsilon_z^2+8g\epsilon_z\epsilon_x\ , \tag{4}$$

$$e_{110}=e_{101}=\hbar\omega_z+\hbar\omega_x-\lambda-2\lambda'-3\lambda'' +12c_{4,z}\epsilon_z^2+12c_{4,x}\epsilon_x^2 +2f\epsilon_x^2+10g\epsilon_z\epsilon_x\ , \tag{5}$$

where ω_z and ω_x are the harmonic frequencies, and we have used the definitions

$$\epsilon_z=\hbar/(2M\omega_z),\quad \epsilon_x=\hbar/(2M\omega_x)\ ,$$

$$\lambda=4\delta/(\hbar\omega_x),\quad \lambda'=4\delta/(-\hbar\omega_z+2\hbar\omega_x)\ ,$$

$$\lambda''=4\delta/(\hbar\omega_z+2\hbar\omega_x)\ .$$

Here M is the hydrogen mass and

$$\delta=-e^2(\hbar/2M)^3/(\omega_z\omega_x^2)\ .$$

The vibrational energies listed in Eqs. (2)–(5) are those appropriate to the levels that could be detected with reasonable confidence in our experimental data.

By suitably combining the above relationships, one can obtain the following expressions for the anharmonicity parameters

$$12c_{4,z}\epsilon_z^2=e_{200}-2e_{100}\ , \tag{6}$$

$$\hbar\omega_z=4e_{100}+e_{010}-e_{200}-e_{110}\ , \tag{7}$$

$$\xi\equiv-\lambda'-\lambda''+4g\epsilon_z\epsilon_x=e_{100}-12c_{4,z}\epsilon_z^2-\hbar\omega_z\ . \tag{8}$$

The first two allow information about the z vibration to be extracted directly. The third allows one to estimate the strength of the anharmonicities coupling the singlet and doublet vibrations.

Since the hydride phases discussed in this work are not bcc structures, it is important to consider the effect of lattice distortions on the results obtained above. The orthorhombic distortion of the bcc lattice for β-NbH_x is small enough so that it can be regarded as a perturbation which affects both the harmonic and the anharmonic models. The perturbation of the anharmonic terms H_1 by the distortion are of higher order than H_1 and will be neglected, while that of the zeroth-order harmonic model is at least of the same order as H_1 and must, therefore, be included. These approximations are implemented by keeping H_1 the same, but using new normal-mode frequencies and displacement directions. By direct calculation, we have found that if the x-y modes are mixed and split, but not mixed with the z modes, Eq. (6) holds exactly, and that Eq. (7) holds if e_{110} is replaced by the average of e'_{101} and e'_{110}, the two slightly different excitation energies which arise in place of e_{101} and e_{110} from the lattice distortion. Similarly, e_{010} must be replaced by $\frac{1}{2}(e'_{010}+e'_{001})$. In our data, such splittings are not resolved, and hence, our measured peak positions are exactly this average and can be used in Eq. (7) without any reduction.

A H-Nb nearest-neighbor (NN) longitudinal spring model for the H local-mode vibration predicts that no mixing of the z with the x and y modes will occur as a result of the β-phase distortion. For H's in those sites occupied in the β phase, the orthorhombic distortion will twist and flatten the tetrahedron formed by the H, its four NN Nb atoms, and the four H-Nb springs.[16] The degenerate modes will, therefore, be split, but not mixed with the z mode. This result may be expected to hold to a good approximation since the NN spring model accounts well for the general features of the H local-mode frequencies.

A final comment concerns the size of the effect of the splitting of the degenerate modes resulting from the orthorhombic distortion in the β phase. If a small splitting of the frequencies and an arbitrary recombination of the displacement vectors is taken, the terms in Eqs. (2)–(5) and (8) that involve ω_x change by a small fraction when the distortion is applied. This change was calculated to be of the order of $\Delta\omega_x/\omega_x$, where $\Delta\omega_x$ is the size of the splitting. For small lattice distortions, therefore, these terms will not be greatly affected. Since such splittings in the doublet are not resolved in the present data, a more quantitative discussion of their effect on the above results is not possible. The middle quantity in Eq. (8) will, therefore, be considered to be only an approximation when the β-phase lattice distortion is present. The experimental value of ξ still measures λ, λ', λ'', and g, but its connection with these quantities is then only roughly given by Eq. (8).

III. EXPERIMENTAL DETAILS

The inelastic neutron scattering experiments were performed on the crystal-analyzer spectrometer (CAS) at the pulsed spallation neutron source (WNR) at the Los Alamos National Laboratory. The WNR at present utilizes about 5 μA of the

800-MeV-proton beam of the Los Alamos Meson Physics Facility. It is therefore only a medium-flux neutron source, but nevertheless has an advantage over reactor-based sources in epithermal neutron flux. The reason for this is that at high energies the neutron flux of a spallation source decreases much more slowly ($1/E$) than that of the Maxwellian spectrum of a reactor. Thus experiments designed to study high-energy excitations such as the harmonics of hydrogen vibrations in metals should have a better chance for success at this type of neutron source.

The CAS is an inverted geometry[17] time-of-flight (TOF) spectrometer designed to study dispersionless high-energy excitations with excellent energy resolution. Since a description of this instrument is not available in the readily accessible literature, we would like to give a short discussion of the particular CAS at the WNR (Fig. 1). In this instrument a "white" neutron beam of 5×10 cm^2 is incident on the sample located 6.4 m from the source. Neutrons scattered in the range of scattering angles $80°<2\theta<107°$ from the planar sample, oriented at an angle of 45° to the incident beam, are then energy-analyzed by an array of six pyrolytic graphite crystals. The crystals are arranged in a time-focused array[18] at 90° to the scattered beam such that all neutrons reaching the detector bank (17 ^{3}He counters, $\frac{1}{2}$-in. diameter) have approximately the same final energy of 3.6 meV and the same flight time from the sample. Higher-order neutrons diffracted by the analyzer array, which would give rise to false, apparently inelastic peaks, are removed by a cooled Be filter, 8 in. long, placed between the analyzer and detector. Neutrons arriving in the detector bank are time sorted into bins 3.2-μsec wide, and by subtracting the fixed final flight time (sample to detector) the incident flight time and the energy transfer to the sample can readily be determined. In the most recent configuration this instrument utilized graphite crystals with mosaic spreads of 0.4° and 1.2° full width at half maximum (FWHM). The resolution of the instrument was calculated using a Monte Carlo computer code due to Sköld and Crawford.[19] With a proton pulse width of 6 μsec FWHM, the resolution varies from about 4% ($\Delta E/E$, FWHM) at an energy transfer of 50 meV to about 7% at 300 meV. Particularly at energy transfers greater than 100 meV the resolution of this instrument is as good or better than reactor-based instruments using the Be-filter technique with Cu monochromator crystals.[20] Moreover, the background in the CAS is structureless, unlike that of instruments using crystal monochromators[3] at high energies where filtering the incident beam is difficult.

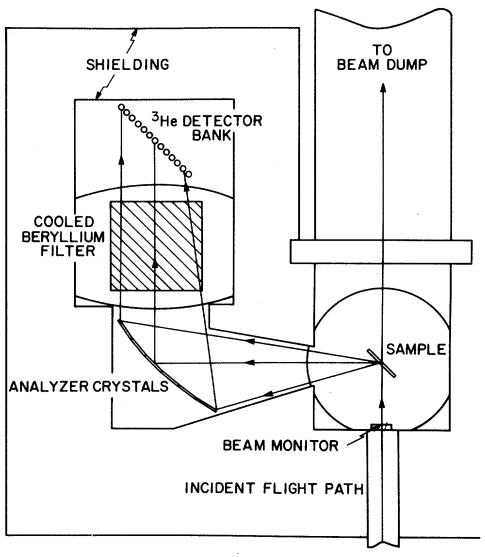

FIG. 1. Crystal analyzer spectrometer at the Los Alamos pulsed spallation neutron source.

The samples were prepared from single-crystal rods of Nb and Ta of $\frac{1}{2}$-in. diameter and various lengths. Before loading with hydrogen or deuterium the crystals were annealed in an ultrahigh vacuum (UHV) at 2300 °C for 24 h in order to remove interstitial impurities. The hydride crystals were subsequently ground up and loaded into flat-plate sample holders for which the CAS is optimized. Counting times for the hydride samples ranged from 12—48 h depending on the amount of material available and the desired precision. Because of the much smaller scattering cross section of deuterium compared with hydrogen, the deuteride sample had to be run for approximately four days. The TOF data were corrected for background and the intensities by the shape of the incident-neutron spectrum as determined by a fission chamber. The data presented in the figures are, therefore, proportional to the scattering function $S(Q,\omega)$.

IV. RESULTS AND DISCUSSION

A. Phase diagram

As was pointed out above, a localized oscillator on a tetrahedral site in a bcc crystal has two excitation frequencies, a singlet at a lower energy corresponding to out-of-plane motion and a degenerate doublet for the in-plane motion. The inelastic neutron scattering spectrum in this case would show two sharp lines, of which the one at higher energy should have twice the integrated intensity of the lower one. In addition, higher harmonics (i.e., $0\rightarrow2$,

$0 \rightarrow 3$, etc. oscillator transitions) corresponding to each fundamental may also be present. For site symmetries lower than tetragonal three lines may occur in the general case. However, as was suggested above for the orthorhombic distortion of β-NbH, such site-symmetry-induced splittings may be too small to be resolved. For a pronounced off-center location of the proton very large effects on the local-mode frequencies have been observed[7] in $VH_{0.51}$. If the protons are distributed over more than one crystallographically inequivalent site, as many as three $0 \rightarrow 1$ oscillator transitions per site may be observed, thereby giving rise to a potentially very complicated spectrum. This may be the situation[6,21] in $FeTiH_x$ where analysis of the neutron scattering spectra is quite complicated.

While in the β-phase of NbH_x only one type of site is occupied[22] by hydrogen, similar information is not known for most of the proposed structures occurring in the low-temperature, high-concentration portion of the phase diagram.[14,23] Limited information is available on the γ phase,[24,25] ξ and ϵ phases,[23,26] and the λ phases.[23,27] In the latter case, long-periodicity superlattices are proposed corresponding to various degrees of ordering of the protons in successive layers. The extent to which such crystallographic changes affect the observed inelastic spectrum of the hydrogen vibrations then depends on the degree to which the local environment of the proton changes. Multiple hydrogen sites, of course, are possible both within a given crystal structure and in cases where two different phases coexist. Since both coherent inelastic neutron scattering studies[8] as well as some recent studies[3,5] using incoherent inelastic scattering suggest that H-H interactions are negligibly small, we will in the following description of our results interpret line broadening or splittings in the low-temperature ordered phases in terms of multiple hydrogen sites as discussed above. The effect of multiphonon scattering is expected to be a broadening around the base of the optic-mode peaks[3] rather than a broadening of the whole peak. Multiple scattering, though probably significant, generally contributes[28] a rather structureless background to the spectra.

Shown in Fig. 2 are the inelastic neutron scattering spectra of $NbH_{0.87}$ at 300 and 78 K, and shown in Fig. 3 are the spectra of $NbH_{0.78}$ and $NbD_{0.80}$ at 78 K. For the purposes of this discussion the spectrum of $NbH_{0.95}$ at 300 K (Fig. 4) may also be referred to. By comparing these figures the following observations may be made: (1) The fundamental excitations in both $NbH_{0.78}$ and $NbD_{0.8}$ are noticeably broadened, (2) reducing the temperature on the sample with composition $NbH_{0.87}$ introduces a noticeable splitting in the local-mode peaks, while (3) this

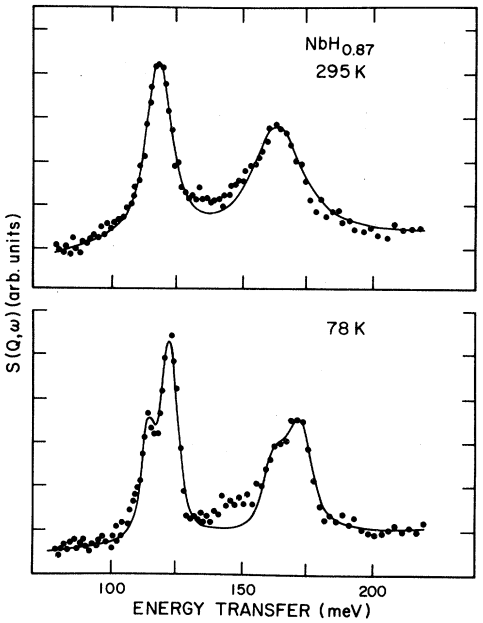

FIG. 2. Inelastic neutron scattering spectrum for $NbH_{0.87}$ reduced to $S(Q,\omega)$. At 295 K, the sample is pure β phase, while at 78 K, the local-mode peaks are split indicating a mixed-phase region (see text). Solid line represents a fit of one Lorentzian for each excitation convoluted with a Gaussian resolution function.

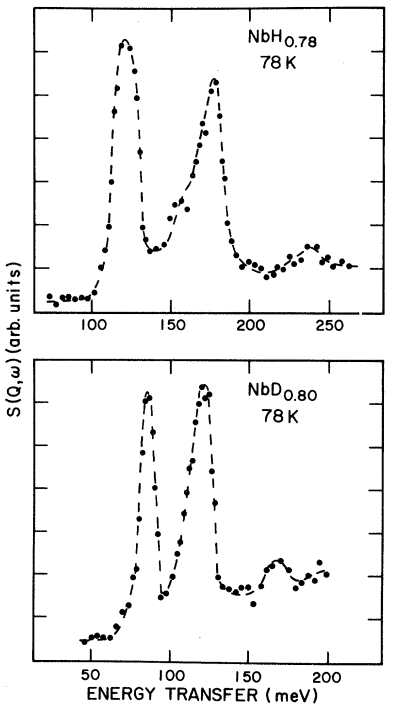

FIG. 3. $S(Q,\omega)$ for $NbH_{0.78}$ and $NbD_{0.80}$. Broadened peaks indicate the presence of multiple H sites, most likely from different phases (see text). Small peaks are e_{200}. Dashed line is a guide to the eye only.

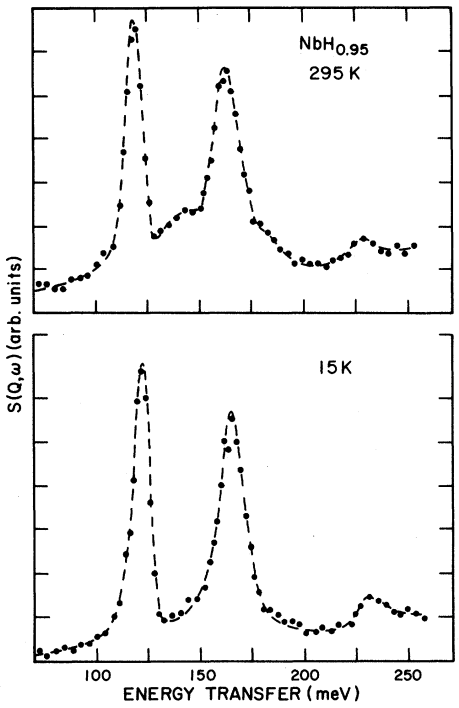

FIG. 4. $S(Q,\omega)$ for $NbH_{0.95}$ at 295 K (β phase) and 15 K ($\beta+\gamma$) phases (Ref. 14).

does not happen in the case of $NbH_{0.95}$. Comparison may also be made with Fig. 1 of Ref. 5 ($NbD_{0.85}$ at 10 K) which also shows nearly resolution-limited peaks.

In order to discuss the differences illustrated in these figures, reference must be made to the NbH_x phase diagram. Since there exist competing versions of the high-concentration, low-temperature portion of this phase diagram, we will first refer the discussion to the work[14] of Köbler and Welter, and subsequently to the alternate version by Birnbaum and collaborators.[23,27] According to the former phase diagram, $NbH_{0.78}$ and $NbD_{0.8}$ at 78 K are in a region where i, O, and ν phases coexist. Also $NbH_{0.87}$ is shown to undergo a transition $\beta\rightarrow(\beta+\nu)$ upon colling below 200 K, followed by further transitions, $(\beta+\nu)\rightarrow(\xi+\beta)\rightarrow(\xi+\gamma)$. $NbH_{0.92}$ and $NbH_{0.95}$ are indicated as undergoing phase transitions from β to $(\beta+\gamma)$ at temperatures well below 200 K. However, further measurements on $NbH_{0.87}$ down to a temperature of 10 K did not produce any further changes in the local-mode spectrum (Table I). From this observation one may then conclude that the local environments of the H sites in the $(\beta+\nu)$ phase-coexistence region do not change noticeably on going through the further transitions mentioned above. This in turn leads to the inference that the ν and ξ phases on the one hand, and the β and γ phases on the other, be very similar. Since both of the samples in the phase-coexistence region $(\beta+\gamma)$ studied in the present work show nearly-resolution-limited lines at low temperature (Table I), the latter part of this conclusion can be further supported. This is not inconsistent with the structural information[24–26] that is available on the γ phase, provided that the relative distortions in the two structures are similar.

The only other inelastic neutron scattering study[5] of the same type as the present work on this portion of the phase diagram is on $NbD_{0.85}$ at 10 K. According to the phase diagram by Köbler and Welter, this sample should be pure ξ phase. The sharp lines observed[5] by Richter and Shapiro, therefore, indicate that the tetrahedral sites in this phase are quite regular. It should also be noted that in the course of performing measurements of acoustic phonons in

TABLE I. Optic-mode energies for NbH_x, $NbD_{0.8}$, and $TaH_{0.71}$. All values in meV. Broadened peaks are analyzed in terms of two sites, indicated as (1) and (2). Phase identification is from Ref. 14. Uncertainties on Γ are typically about 1 meV.

Sample	Phase(s)	T (K)	e_{100} (1)	e_{100} (2)	Γ_{100}	e_{010} (1)	e_{010} (2)	Γ_{100}
$NbH_{0.78}$	i,O	78	118.3(9)	126.1(9)		167(2)	177(2)	
$NbD_{0.80}$	i,O,ν	78	84.8(8)	88.6(8)	3	116.9(1.5)	124.4(1.5)	4
$NbH_{0.87}$	β	300	119(1)		4.2	164(1.5)		12.4
$NbH_{0.87}$	$\nu+\beta$	193	114(1)	123(1)	3.3	163(2)	172(2)	5.8
$NbH_{0.87}$	$\xi+\beta$	150	115(1)	123(1)	3.0	163(2)	173(2)	5.2
$NbH_{0.87}$	$\xi+\gamma$	78	115(1)	124(1)	1.3	165(1.5)	174(1.5)	4.2
$NbH_{0.92}$	β	300	118(1)		4.4	162(2)		9.9
$NbH_{0.92}$	$\beta+\gamma$	78	120(1)		3.5	163(1.5)		6.6
$NbH_{0.95}$	β	300	118(1)		4.5	163(2)		9.5
$NbH_{0.95}$	$\beta+\gamma$	150	121(1)		3.6	165(1.5)		6.8
$NbH_{0.95}$	$\beta+\gamma$	15	121.8(8)		3.0	165.6(1.5)		6.0
$TaH_{0.71}$	ζ	78	130(1)		3	170(2)		6

this sample, Shapiro *et al.*[29] detected a phase transition at 203 K. They indicated that the observations made on this new phase were not consistent with published information on the γ phase, which they thought the sample had entered. However, according to the new phase diagram,[14] $NbD_{0.85}$ passes through a region of $\nu+\beta$ coexistence at 203 K before transforming to the ξ phase.

Other work[30,31] on this portion of the NbH_x phase diagram is considerably less complete than that by Köbler and Welter[14] and in some details[30] in disagreement with the latter. It is, therefore, not possible to relate our observed local-mode line shapes in as much detail to those phase diagrams. A few comments may, however, be made relative to the λ phases found by Birnbaum and collaborators.[23,27] At least three different such phases are proposed to cover the concentration ranges H to Nb of 0.72—0.77, 0.85—0.90, and 0.91—0.96. The λ structures are based on stacking of different variants of orthorhombic β-phase unit cells along the [001] axis of the cubic α' cell. In some cases, these phase layers can be viewed as being separated by boundary layers of ζ phase. Superimposed on this stacking is a hydrogen density wave which results in additional superlattice reflections. These structures cannot be related to the pseudocubic γ phase, and no evidence thereof was found[23] by Makenas and Birnbaum.

As far as the effect of such modulated structures on the hydrogen local-mode spectrum is concerned, one can only make qualitative observations since the details of the γ-phase structures (such as interatomic distances) are not known. Depending on the periodicity of the structure, a large number of inequivalent H sites are possible. The degree to which each of these sites would give rise to different local-mode frequencies would then depend on the effect of the H-sublattice ordering on the positions of the Nb atoms, i.e., the degree to which the NN H-Nb distances differ for the inequivalent sites. One might expect a distribution of H sites, each with slightly different local environments, which would then simply broaden the optic-mode peaks. In a recent theoretical calculation[32] Sugimoto and Fukai conclude that a displacement of the NN metal atoms of a proton of only 2% would give rise to a broadening of the local-mode peaks by about 30 meV. While this seems somewhat more than present measurements indicate, it does suggest that in a situation where many different H sites exist, large linewidths could be expected. The data on $NbH_{0.78}$ and $NbD_{0.80}$ obtained in the present work is not incompatible with the above results on the λ phases, nor with a simple coexistence of two different phases, particularly since no structure is resolved in the local-mode peaks. The splittings observed on the $NbH_{0.87}$ sample, however, indicate a two-phase coexistence in agreement with the phase diagram by Köbler and Welter,[14] while in the case of the λ phases broad peaks would be expected.

The existing phase diagrams[30] for TaH_x seem to agree that our $TaH_{0.71}$ sample should be nearly pure ζ phase. The fits to the data do indeed result in relatively small intrinsic widths (Table I), and are, therefore, in qualitative agreement with the phase diagram. Note should also be made of the higher energies observed for this sample when compared with more dilute samples studies by other authors.[31,33] The values obtained in the present work, 130 and 170 meV for the fundamentals, are significantly larger than those[3] for β-$TaH_{0.08}$, 121 and 163 meV. This dependence of the local-mode frequencies on concentration is in agreement with the work[33] by Watanabe and Furusaka, who found essentially no concentration dependence at room temperature up to $x=0.50$ followed by a steady increase for concentrations greater than that value. For $TaH_{0.69}$ at 20°C, they find energies of approximately 128 and 169 meV, in good agreement with the present results. A similar comparison for data on NbH_x does not show as much of a concentration dependence, namely[4] 116 and 166 meV for β-$NbH_{0.14}$ as opposed[5] to 119 and 167 meV for β-$NbH_{0.82}$. Presumably, these differences between the NbH_x and TaH_x systems are related to their respective phase diagrams, but it is not possible to make more than qualitative comments on this question for lack of more detailed data. Differences in their electronic structures may be expected to play a role as well.

In order to gain more information on the H-Nb interaction from these measurements, it is essential to have complete crystallographic data available from all the regions of the NbH_x phase diagram. Once the details of the hydrogen sites in the various phases are known, it should be possible to analyze the present data in a consistent way to determine differences between the various phases. With few exceptions,[22] the structural information on the NbH_x phases is quite incomplete at present.

B. Anharmonicity

The simple anharmonic model presented in Sec. II has been used to analyze the data on the higher harmonic transitions and combination bands shows in Table II. Some of this experimental data is also shown in Fig. 5 with fits (Lorentzian convoluted with Gaussian resolution) indicated by solid lines. In most cases, a peak corresponding to the $0\rightarrow 2$ transition of the singlet vibration could be clearly discerned. In addition, intensity due to higher tran-

TABLE II. Higher harmonic transitions in NbH_x, $NbD_{0.8}$, and $TaH_{0.71}$. All values in meV. For coexistent phases weighed average values are used.

Sample	Phase(s)	T (K)	e_{100}	e_{010}	e_{200}	e_{110}
$NbD_{0.80}$	i,O	78	86.7(9)	120.7(9)	166(3)	205(5)
$NbH_{0.78}$	i,O,ν	78	120(1)	169(2)	233(3)	
$NbH_{0.87}$	$\xi+\gamma$	78	120(1)	169(2)	230(3)	
$NbH_{0.92}$	β	300	118(1)	162(2)	227(3)	273(6)
$NbH_{0.92}$	$\beta+\gamma$	78	120(1)	163(2)	227(2)	277(5)
$NbH_{0.95}$	$\beta+\gamma$	150	121(1)	165(2)	230(2)	278(5)
$NbH_{0.95}$	$\beta+\gamma$	15	122(1)	166(2)	231(2)	280(4)
$TaH_{0.71}$	ζ	78	130(1)	170(2)	245(3)	

sitions is also evident in some spectra, but it is difficult to assign reliable peak positions in these cases. Nevertheless, attempts were made to extract energies for the combination band (i.e., a simultaneous excitation of the singlet and doublet modes) as it is a direct measure of the degree of coupling between the x, y, and z motions of the proton. The structure above 300 meV that may be recognized in some spectra (Fig. 5) would be due to both the $0\rightarrow 3$ transition of the singlet and $0\rightarrow 2$ transition of the doublet vibrations. Unfortunately, these are neither resolved nor of sufficient intensity to extract useful information thereof. Thus, only peak positions that could be discerned with reasonable accuracy are given in Table II.

The three-dimensional anharmonic-oscillator model developed in Sec. II can now be used to analyze some of the data shown in Table II. In the following discussion, only data on β-phase and mixed- $(\gamma+\beta)$ phase samples will be used, since

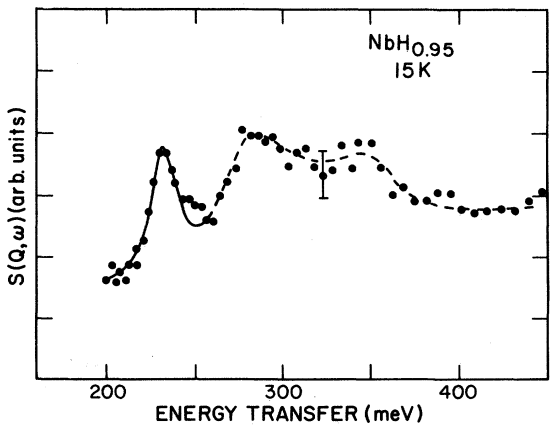

FIG. 5. Higher harmonics for $NbH_{0.95}$ at 15 K. Solid line represents a fit through e_{200}. Dashed line is a guide to the eye for the broad band consisting of e_{110}, e_{020}, and e_{300}, most likely in this order.

mixed-phase samples of other compositions either have strong broadening or structure in the local-mode peaks. For the β and γ phases, however, it appears (see Fig. 4) that the H vibrations are very similar as the observed peaks have widths that are close to being resolution limited. Some structural evidence[22,24] on the γ phase further supports this assumption, since in the pseudocubic phase no vibrational-mode mixing or splitting would be expected to occur.

It is most convenient to make use of Eqs. (6)—(8) to determine the anharmonic parameters from the experimental data. First, values of $12c_{4,z}\epsilon_z^2$ are obtained using Eq. (6) yielding -9, -13, -12, and -13 meV, respectively, for the samples $NbH_{0.92}$, $NbH_{0.95}$, and $NbH_{0.95}$ at temperatures 300, 78, 150, and 15 K, respectively. The corresponding values of $\hbar\omega_z$ obtained using Eq. (7) are 134, 139, 141, and 143 meV, respectively. Equation (8) then gives results for ξ of -7, -6, -8, and -8, respectively. In each of the cases the values for the different samples are reasonably consistent with each other, and show that both $12c_{4,z}\epsilon_z^2$ and ξ are about equally important contributors to the anharmonicity. Thus, the earlier interpretation[5] of the anharmonic effect on the lower fundamental in terms of a one-dimensional potential omitted the anharmonic coupling to the x-y vibrations. This approach is hereby shown to be valid only if $\xi \ll 12c_{4,z}\epsilon_z^2$.

In an effort to include isotope shifts in the present discussion, the data on the presumably mixed-phase samples $NbD_{0.80}$ and $NbH_{0.78}$ (both at 78 K) were analyzed with the anharmonic theory of Sec. II despite the obvious broadening (Fig. 3) of the local-mode peaks. These equations, of course, do not necessarily apply in the presence of several inequivalent H sites and thereby different local-mode vibrations.

In addition, vibrational-mode mixing between the z mode and the x,y modes cannot be ruled out since no information on the local geometry in the i, O,

and ν phases is available. For the deuteride sample, we obtain for $\hbar\omega_z$, $12c_{4,z}\epsilon_z^2$, and ξ, the values 96.5, -7.4, and -2.4 meV, respectively. Using these values, one can make the model predictions for hydride values of $\hbar\omega_z$, $12c_{4,z}\epsilon_z^2$, and ξ since our model gives these quantities mass dependences of $1/\sqrt{M}$, $1/M$, and $1/M$, respectively. The values of 136.5, -14.8, and -4.8 meV thus obtained compare well with the values 139, -13, and -6 meV obtained with our equations from data of the $NbH_{0.92}$ sample at 78 K. As the value of e_{110} for $NbH_{0.78}$ could not be determined in the present experiment, a comparison with this prediction can only be made for $12c_{4,z}\epsilon_z^2$ for which this data yields -7 meV. This value does not agree well with the value predicted above from the deuteride data, which is really not surprising for the reasons stated above. We note, in passing, that the $12c_{4,z}\epsilon_z^2$ value obtained for $NbD_{0.80}$, -7.4 meV, agrees well with the -6.6 meV determined earlier[5] for $NbD_{0.85}$ at 10 K.

For $TaH_{0.71}$ at 78 K, the parameter $12c_{4,z}\epsilon_z^2$ was found to be -15 meV, in good agreement with the data[3] on β-$TaH_{0.08}$ at 77 K of -15.5 meV. In addition, this value is close to those for $NbH_{0.87}$, $NbH_{0.92}$, and $NbH_{0.95}$, which suggests that the degree of anharmonicity in NbH_x is comparable with that in TaH_x at least as far as the z vibration is concerned.

In a recent inelastic neutron scattering study[4] local-mode frequencies were reported for the following isotopes of the Nb-hydride system at room temperature: $NbH_{0.32}$, $NbD_{0.725}$, and $NbT_{0.2}$, all of which are then expected to be in the pure β phase. We fitted the hydride and deuteride singlet data to the form

$$\alpha/[(M/M_H)]^{1/2}+\beta/(M/M_H)\ ,$$

where α and β are mass independent, and obtained a value of 135.2 meV for α and -19.2 meV for β. We can then use these α and β values to *predict* a tritide-singlet fundamental frequency of 71.7 meV which compares rather well with the experimental value of 72 meV. We must note, however, that the experimental uncertainties quoted with the vibrational data make the above calculated values uncertain by roughly 5% for α and 40% for β. The same procedure for the doublet frequencies yielded a calculated tritide-doublet frequency differing by only 2.3% from the experimental one. The success of this simple isotope-effect formula strongly suggests that the same potential is encountered by all three isotopes, at least as far as e_{100} and e_{010} are concerned. The value -19.2 meV for β, which is a measure of the total anharmonicity present, compares favorably with the total calculated anharmonic part of e_{100} for $NbH_{0.92}$ (300 K), $NbH_{0.92}$ (78 K), $NbH_{0.95}$ (150 K), and $NbH_{0.95}$ (15 K), namely -16, -19, -20, and -21 meV, respectively. This agreement strengthens the case that our anharmonic model applies to the β phase and the other β-like phases involved in these systems.

V. CONCLUDING REMARKS

The above discussion has demonstrated that when measurements of the vibrational frequencies of hydrogen in metals include a large enough number of transitions, as well as their isotope effect, and are combined with an appropriate theoretical model, valuable information on the anharmonicities of the metal-hydrogen potential can be obtained. This is particularly true in cases where the inelastic lines are sharp and the crystal structure including site symmetries is known. Thus, most of the data on β-phase NbH samples, both from the present work and from that of previous authors, could be analyzed in a consistent fashion by our anharmonic-oscillator model. This then allowed the conclusion that the potential for the different isotopes H, D, and T in the β-hydride phase of Nb appears to be the same.

For hydrides in the other regions of the very complicated phase diagram at large concentrations and low temperatures, the data cannot be quantitatively interpreted because of the apparent presence of multiple hydrogen sites, which are presumed to correspond to different hydride phases. As was pointed out above, detailed crystal-structure data on these phases is urgently needed. Little progress can be expected in the understanding of the phase transitions occurring in this portion of the phase diagram if such data is not available. The present inelastic neutron scattering measurements (Figs. 2 and 3) show the relative sensitivity of hydrogen to changes in its environment and how, therefore, in a qualitative way such data can be used to observe phase changes in a metal hydride. This was also pointed out[21] by Shapiro *et al.* in their work on $FeTiH_x$, in which the inelastic data is still more difficult to interpret than in the present case. It should be emphasized, however, that structural data in any case is essential for the extraction of the maximum amount of information from these measurements such as by lattice dynamical modeling.

For future applications of neutron vibrational spectroscopy on metal hydrides, it may well be desirable to do the measurements with higher accuracy at large-energy transfers. While we have for the first time been able to observe transitions in a bcc hydride at energies greater than 300 meV, the counting statistics in this measurement are not good

enough to separate, e.g., the $0\rightarrow 3$ singlet and $0\rightarrow 2$ doublet transitions. This should be possible with the new high-intensity pulsed neutron sources such as the upgraded WNR at Los Alamos which is expected to come on line in the next few years. At that point, more stringent tests of theoretical models will be possible. Particularly the question of a possible isotope effect on the hydrogen potential is of considerable interest. More extensive measurements that involve deuterated and tritiated Nb of the same concentrations as the hydride in question are needed to clarify this question. Unlike in the case of the VH-D system where a strong isotope effect on the phase diagram is well known and connected with differences in site occupation of H and D, most of the available information[22] on the NbH-D system suggests little or no isotope effect on the phase diagram. Recently, however, Schober[30] did point out the existence of a pronounced isotope effect on the transition temperatures $\beta\rightarrow\beta+\alpha'\rightarrow\alpha'$ for H-to-metal ratios greater than 0.5. Finally, it may be anticipated that careful studies of the hydrogen dynamics in Nb as a function of temperature may yield considerable information on the phase transitions occurring in the NbH_x system, particularly in cases where crystal structures of the phases in question are well known.

ACKNOWLEDGMENTS

The authors would like to thank S. M. Shapiro, J. J. Rush, R. Hempelmann, and F. Reidinger for helpful discussions, H. S. Bierfeld for the preparation of the samples used in these experiments, and R. K. Crawford for providing the computer program for calculating the CAS energy resolution. This work was supported in part by the Division of Basic Energy Sciences, U. S. Department of Energy.

---

[1]Preliminary reports on some portions of this work have been presented at the Miami International Symposium on Metal Hydrogen Systems, Miami Beach, Florida, 1981, and the International Symposium on the Electronic Structure and Properties of Hydrogen in Metals, Richmond, Virginia, 1982 [J. Less-Common Metals (in press)].

[2]For a recent review see T. Springer, in *Hydrogen in Metals I,* Vol. 28 of *Topics in Applied Physics,* edited by G. Alefeld and J. Völkl (Springer, New York, 1978).

[3]R. Hempelmann, D. Richter, and A. Kollmar, Z. Phys. B 44, 159 (1981).

[4]J. J. Rush, A. Magerl, J. M. Rowe, J. M. Harris, and J. L. Provo, Phys. Rev. B 24, 4903 (1981); Bull. Am. Phys. Soc. 26, 337 (1981).

[5]D. Richter and S. M. Shapiro, Phys. Rev. B 22, 599 (1980).

[6]J. Eckert, J. A. Goldstone, and D. Richter, J. Phys. F 11, L101 (1981).

[7]D. Klauder, V. Lottner, and H. Scheuer, Solid State Commun. 32, 617 (1979).

[8]V. Lottner, A. Kollmar, T. Springer, W. Kress, H. Bilz, and W. D. Teuchert, in *Lattice Dynamics,* edited by M. Balkanski (Flammarion, Paris, 1978), p. 247; N. Stump, G. Alefeld, and D. Toechetti, Solid State Commun. 19, 805 (1976).

[9]J. M. Rowe, J. J. Rush, H. G. Smith, M. Mostoller, and H. E. Flotow, Phys. Rev. Lett. 33, 1297 (1974).

[10]C. J. Glinka, J. M. Rowe, J. J. Rush, G. G. Libowitz, and A. Maeland, Solid State Commun. 22, 541 (1977).

[11]P. Vorderwisch, S. Hautecler, and W. Wegener, J. Less-Common Met. 74, 117 (1980).

[12]G. Herzberg, *Spectra of Diatomic Molecules* (Van Nostrand, New York, 1950), p. 93.

[13]R. Yamada, N. Watanabe, K. Sato, H. Asano, and M. Hirabayashi, J. Phys. Soc. Jpn. 41, 85 (1976).

[14]U. Köbler and J. M. Welter, J. Less-Common Met. 84, 225 (1982).

[15]M. Tinkham, *Group Theory and Quantum Mechanics* (McGraw-Hill, New York, 1964).

[16]M. A. Pick and R. Bausch, J. Phys. F 6, 1751 (1976).

[17]A. Bajorek, T. A. Machekina, K. Parlinski and F. L. Shapiro, in *Inelastic Scattering of Neutrons 1964* (IAEA, Vienna, 1965), Vol. II, p. 519.

[18]K. Sköld, R. K. Crawford, and S. M. Chen, Nucl. Instrum. Methods 145, 91 (1977).

[19]R. K. Crawford and K. Sköld (private communication).

[20]Institut Maxvon Laue—Paul Langevin (ILL) Manual, *The Neutron Beam Facility and Instrument Specifications* (Institut Max von Laue—Paul Langevin, Grenoble, 1977).

[21]S. M. Shapiro, F. Reidinger, and J. F. Lynch, J. Phys. F 12, 1869 (1982).

[22]T. Schober and H. Wenzl, in *Hydrogen in Metals II,* Vol. 29 of *Topics in Applied Physics,* edited by G. Alefeld and J. Völkl (Springer, New York, 1978).

[23]B. J. Makenas and H. K. Birnbaum, Acta Metall. 30, 469 (1982).

[24]M. A. Pick, Ph.D. thesis, Technische Hochschule Aachen, Germany, 1973 (unpublished).

[25]J. A. Hauck, Acta Crystallogr. A 33, 208 (1977).

[26]T. Schober, Phys. Status Solidi A 30, 107 (1975).

[27]T. O. Brun, T. Kajitani, M. M. Mueller, D. G. Westlake, B. J. Makenas, and H. K. Birnbaum, in *Modulated Structures—1979 (Kailua Kona, Hawaii,* Proceedings of the International Conference on Modulated Structures, edited by J. M. Cowley, J. B. Cohen, M. B. Salamon, and B. J. Wuensch (AIP, New York, 1979), p.

397.
[28]W. L. Whittemore, in *Inelastic Scattering of Neutrons in Solids and Liquids 1964* (IAEA, Vienna, 1965), Vol. II, p. 305.
[29]S. M. Shapiro, D. Richter, Y. Noda and H. Birnbaum (unpublished).
[30]T. Schober, Proceedings of the International Symposium on the Electronic Structure and Properties of Hydrogen in Metals, Richmond, Virginia, 1982 [J. Less-Common Met. (in press)].
[31]V. A. Melick-Shakhnazarov, I. N. Bydlinskaya, I. A. Naskidashvili, N. L. Arabadzhyan, and R. V. Chachanidze, Zh. Eksp. Teor. Fiz. 81, 317 (1981).
[32]H. Sugimoto and Y. Fukai, J. Phys. Soc. Jpn. 50, 3709 (1981).
[33]N. Watanabe and M. Furusaka (unpublished).